



Design and fabrication of an electrical glider to compare theoretical and experimental parameter

Hari Sharan Dangia*, Prabij Joshi^a, Dinesh Tamang^a, Munna Chauhan Mahato^a,
Nabin Bhattarai^a, Ram Tripathi^a and Bishal Poudel^a

^aDepartment of Mechanical and Automobile Engineering, Paschimanchal Campus, Tribhuvan University, Nepal

ARTICLE INFO

Article history:

Received 25 August 2024
Revised in 29 September 2024
Accepted 13 October 2024

Keywords:

Aerodynamic
Endurance
Surveillance
Simulation
Unmanned Aerial Vehicle

Abstract

The use of Unmanned Aerial Vehicles (UAVs) is growing rapidly across many civil application domains, including real-time monitoring, wireless coverage, remote sensing, search and rescue, delivery of goods, security and surveillance, precision agriculture, and civil infrastructure inspection. Nepal, being one of the richest countries in natural resources, faces challenges daily to conserve them. With the vision of conservation and surveillance, there is a need for efficient UAVs that can replace ordinary multi-propeller drones. This project has been designed to serve the similar purpose of surveillance and agricultural growth that contribute to the technical field of the nation and promote the development of UAVs within the country. The project focuses on the design, fabrication, and testing of an efficient glider with the use of a lightweight polystyrene foam fuselage, brushless motor, propeller, servo motor, and Lithium-ion Polymer (LiPo) battery for high endurance limit. XFLR software will be used for the wing profile selection and calculation of the drag and lift coefficient, while SOLIDWORKS and ANSYS will be used for the design, simulation, and analysis of the proposed glider. The stall point for the proposed glider was found to be at a 14-degree angle of attack. The total weight of the UAV was about 800 grams with a payload of about 200 grams with a factor of safety 1.8. The glide ratio of the UAV was also compared with the theoretical glide ratio, which was found close to 3.5:1. The endurance limit of the battery was found to be about 9 minutes under-loading.

©JIEE Thapathali Campus, IOE, TU. All rights reserved

1. Introduction

Unmanned Aerial Vehicles (UAVs) have been referred to in many ways as RPVs (Remotely Piloted Vehicles), drones, robot planes, and pilotless aircraft. Most often called UAVs, they are defined by the Department of Defense (DoD) as powered, aerial vehicles that do not carry a human operator, use aerodynamic forces to provide vehicle lift, can fly autonomously or be piloted remotely, can be expendable or recoverable, and can carry a lethal or nonlethal payload. UAVs range from the size of an insect to that of a commercial airliner. The earliest recorded use of a UAV dates to July 1849, when it served as a balloon carrier. However, significant development of drones started in the early 1900s and was used as targets for the training of military per-

sonnel. The earliest attempt at a powered UAV was made by A. M. Low's "Aerial Target" in 1916. The first-ever successful monoplane UAV flight flew under control on 21 March 1917 by Geoffrey de Havilland. Especially concerned about losing the pilot over hostile territory, many powerful countries began planning for the use of un-crewed aircraft that would carry an explosive payload to a predetermined target. Several historical events highlight the development of the UAVs that continued before and after World War I and World War II, primarily used for flying attack missions which later contributed significantly to the growth and development of drones. Later, as the technology grew, there was massive use of cameras, trackers, and sensors in the UAVs. Presently, with the maturing and miniaturization of technologies, UAVs are well-equipped with different electronic instruments and are used in numerous civil, commercial, agriculture, military, and aerospace applications [1].

*Corresponding author:

 harrysharandc84@gmail.com (H.S. Dangia)

2. Objectives

- To design and develop an efficient fixed-wing UAV with a single propeller configuration and test the performance.
- To study the glide ratio.
- To study the drag and lift force.
- To study horizontal flight capabilities.
- To study the possibility of a safe landing without the use of energy but using its gliding property only.
- To test the fabricated model and analyze the results.

3. Literature review

Moore, 2010, Aircraft design variety potential and simplicity is increased with the fact that thrust developed by electric motors is more quickly varied, eliminating the need for complex and heavy variable pitch propellers to achieve the same effects [2].

Lance W. Traub, 2011 brought the concept of battery dumping for an electric powered UAV and using the gliding properties thereafter. Also presented the impact of dumping on the performance parameters. This concept is utilized for the proposed glider, that the gliding ratio of the glider will be used for increasing the battery efficiency by turning the battery off [3].

Aris Sunantyo and his team 2014, bring the concept of the Digital Elevation Model to determine the available Head Assessment for Micro Hydro Power Plant at Banjarnegara District. The team established Ground Control Points (GCP) for vertical and horizontal positioning in carrying out aerial mapping with UAV technology. The available head was determined by the terrestrial or aerial photogrammetric method. The major concern of the project is that the proposed prototype could hold the weight of surveillance cameras to be used in conservation areas [4].

Ngo Khang Hieu et al, 2015 study about different free software for the selection of appropriate and efficient airfoils for small unmanned aerial vehicles. This research presents the XFLR software to be the best free software available for the appropriate airfoil selection for small UAVs. The same XFLR software will be used for the airfoil selection of the main wing, tail wing, and vertical stabilizer [5].

Chang, Tan; Yu, and Hu 2015, presented research to extend electric-powered UAVs' endurance by dumping exhausted batteries out of the aircraft in flight for the higher efficiency of the battery. This approach can also

be considered while designing the proposed prototype for the study of gliding nature by decreasing the speed of the motor [6].

Abdulla Alshehha et al, 2017 in UAE study for the design of a gliding plane in a low-density Martian atmosphere as an alternative to VTOL drones. This research aims to analyze the aerodynamic performance by simulating an airplane gliding the Martian atmosphere through Computational Fluid Dynamics simulations. The analysis will be performed to assess the flow-field environment around the gliding airplane in the Martian atmosphere considering that Mars has a lower gravity than Earth, thinner air at the surface, and the major component of Mars' air is CO₂ gas which is denser than Earth's air for a given pressure. The study addresses the aerodynamic performance of a gliding airplane that includes lift, drag coefficients, glide ratio, weight the glider can carry at varying angles of attack, and velocities. Relating to this concept, the performance of the glider will be computed for the different angles of attack, velocities, and other boundary conditions to use this glider as an alternative to conventional VTOL drones [7].

Alan G. Escobar-Ruiz et al, 2019 presented a research paper focusing on the aerodynamics and design of an unmanned aerial vehicle (UAV) based on solar cells as the main power source during cruising and the use of batteries during take-off. A conceptual design was used, and the aerodynamic analysis was focused on a UAV as a gliding vehicle, with the calculations starting with the estimation of weight and aerodynamics and finishing this stage with the best glide angle. The aerodynamic analysis was obtained for a preliminary design; this step involves the wing, fuselage, and empennage of the UAV. The major concern of the project will be to make the glider take off from the ground and also to increase the efficiency by using the gliding property turning the motor off when it reaches its maximum height [8].

Keskin, Göksel & Durmus, Seyhun & Kafali, Haşim, 2019, at Budapest research on the replacement of internal combustion engines with electric powered motors during take-off to make a glider self-launched. In this work, the history of the motor glider, differences between engine options, and advantages of the electric engines were evaluated for gliding sport. This approach will be used by installing a battery as the driving force [9].

Karthik Balajee Laksham, 2019 used the concept of using unmanned aerial vehicles for the supply of medicines, antibiotics, vaccines, blood, and other emergency medical things. The main objective of this project is also to increase the payload capacity of the glider so that the maximum load can be supplied using the glider

for emergency purposes [10].

Kozuba, Jaroslaw & Wojnar, 2021 at the Silesian University of Technology presented an electric-powered glider for take-off only and the use of self-gliding to increase the level of safety of glider flight by enabling the use of propulsion at critical moments of the flight. The study presents the current trends in the development of gliding, in particular motor gliders. Concerning this approach, the main objective of the proposed project will be to increase the efficiency of the overall prototype by turning the motor off when it reaches its maximum height [11].

4. Methodologies and materials

4.1. Design methodology

The following flow diagram shows the design methodology of the project. The UAV design process is also similar to the general design process. However, there are some additions to the design guidelines because the UAV design must pass through various tests and quality certifications so that the final product meets the project requirement.

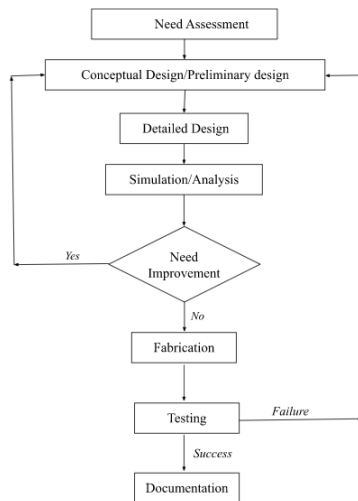


Figure 1: Design methodology

4.2. Software used

XFLR5, SolidWorks, ANSYS are used for the selection of airfoil, for the design of our prototype, and for the analysis.

4.3. Material selection

A critical parameter in the design of a UAV is the choice of material. Ideally, the lightest material and robust against mechanical (drop, shock) and environment (waterproof, salt spray compliant, altitude /low pressure,

oil/chemical contamination/corrosion) shall be selected to ensure the UAV is robust and can be used in any kind of application/situation.

Table 1: Table for the material properties

Material	Density (g/cm ³)	Tensile Strength (MPa)
Polystyrene Foam	0.025	1.35
Aluminum Tubes	2.7	90
PVC	1.38	52

4.4. Design of the glider

4.4.1. Airfoil selection

For the selection of the best airfoil, the drag and lift coefficients of different airfoils were analyzed and among them, the airfoil with a linear increase in coefficient of lift and coefficient of drag was selected.

1. **Main Wing:** The wing is designed with a NACA 4415 asymmetric airfoil, as shown in the Figure 2. It has a maximum thickness of 14.99% at 30.30% chord and a maximum camber of 4.01% at 40.4% chord [12].

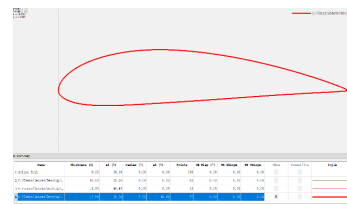


Figure 2: Cross-section of NACA4415

2. **Tail Wing and Vertical Stabilizer:** The wing is designed with a NACA 0012 symmetrical airfoil, as seen in the Figure 3. It has a maximum thickness of 12% at a 29.9% chord and a maximum camber of 0% [13].

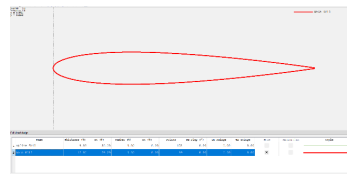


Figure 3: Cross-section of NACA0012

4.4.2. Detail design of the glider in different software

The prototype of the Glider is first designed in the XFLR and SOLIDWORKS with the following spec-

ifications.

1. **Main Wing Design:** The design parameters for the design of the main wing are given in Table 2.

Table 2: Design parameters for the main wing

Design Parameters	Dimensions
Wing Span	120 cm
Wing Area	0.18 m ²
Mean Aerodynamic Chord	15 cm
Aspect Ratio	8
Taper Ratio	1
Sweep Angle	0-degree

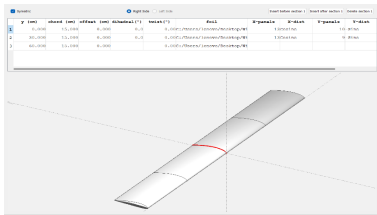


Figure 4: Main wing design in XFLR

2. **Tail Wing or Elevator Design:** The design parameters for the design of tail wing are given in Table 3:

Table 3: Design parameters for tail wing

Design Parameters	Dimensions
Wingspan	40 cm
Wing Area	0.04 m ²
Mean Aerodynamic Chord	10 cm
Aspect Ratio	4
Taper Ratio	1
Sweep Angle	0 degree

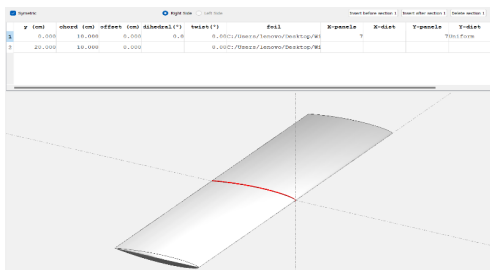


Figure 5: Tail wing design in XFLR

3. **Vertical Stabilizer Design:** The design parameters for the design of a vertical stabilizer are given in Table 4

Table 4: Design parameters for vertical stabilizer

Design Parameters	Dimensions
Wingspan	20 cm
Wing Area	0.02 m ²
Mean Aerodynamic Chord	10 cm
Aspect Ratio	3
Taper Ratio	1
Sweep Angle	0

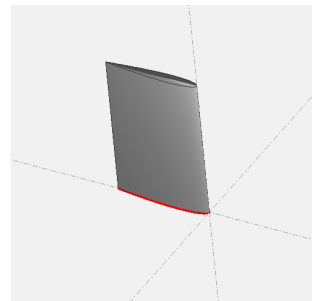


Figure 6: Vertical Stabilizer

4. **Fuselage Design in XFLR:** The fuselage was also designed in XFLR software for the calculation of the position of different electronics components and the C.G. of the glider.
5. **Fuselage Design in SolidWorks:** The design parameters for the fuselage are:

Table 5: Design Parameters for fuselage

Parameters	Dimensions
Length of the Housing	40 cm
Width of the Fuselage	9 cm
Height of the Fuselage	9 cm
Length of Aluminum Rod	80 cm

6. **Assembly in SolidWorks:** The fuselage, main wing, tail wing, and vertical stabilizer were assembled in SolidWorks assigning the respective masses. The mass of individual components is measured with the help of SolidWorks. These masses of individual components are used for the calculation of C.G.

Table 6: Table of the weight of components

Components	Mass (gram)
Fuselage	95
Main Wing with Flappers	90
Tail Wing	10
Vertical Stabilizer with Rudder	10

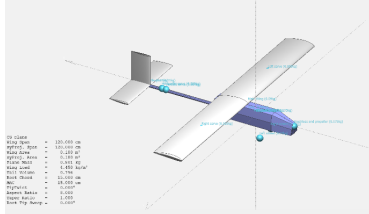


Figure 7: Position of different components in the Glider using XFLR

4.5. Position of different components with their masses

For the measurement of the position of different components, the origin point is taken as the (40, 0, -4.50) cm from the nose of the glider. The position is measured in all three axes because of the 3D arrangement of various components. The components are considered as the point masses for the ease of calculation of C.G.

Table 7: Position of different components with their masses

S.N.	Components	Mass (gram)	X (cm)	Y (cm)	Z (cm)
1	Right Servo	9	11	30	5
2	Left Servo	9	11	-30	5
3	Horizontal Stabilizer Servo	9	49	0	0
4	Vertical Stabilizer Servo	9	47	0	0
5	Battery	325	1	0	0
6	Main Wing	90	4	0	5
7	Tail Wing	10	55	0	0
8	Fuselage	95	0	0	0
9	Vertical Stabilizer	10	55	0	0
10	Brushless Motor and Propeller	75	-20	0	0
11	ESC	25	0	0	0
12	Receiver	15	0	0	0
13	Left Wheel	10	-5	5	-8
14	Right Wheel	10	-5	-5	-8
15	Miscellaneous	100	0	0	0
Total Mass of Glider		801			

4.6. Location of aerodynamic center of gravity

The Center of Gravity should be located at the position slightly ahead of the center of pressure (about 33% from the line of the leading edge) for the higher stability flight of the glider. Using XFLR software, assigning masses of different components and their position the theoretical C.G of the Glider was found as shown in Table 8.

Table 8: Position of C.G from the origin and moment of inertia about a different axis

X (cm)	Y (cm)	Z (cm)	Ixx (kg.m ²)	Iyy (kg.m ²)	Izz (kg.m ²)
3.848	0	0.633	0.01309	0.02037	0.03248

In the Table 8, the C.G. is located at the position near the leading edge (1.5mm) of the main wing along the longitudinal direction and the position 0.633cm above the origin in the vertical direction. This location of C.G. is acceptable for the further design of the glider. The Center of mass is located slightly ahead of the center of pressure which is better for the higher stability of the proposed UAV.

4.7. Fabrication and assembly

The following steps were involved in fabricating the Electrical Glider:

- Initially, the blocks of Styrofoam were cut into the required size using the hot wire cutting method. The frame for the wing airfoil was cut using plywood in a grinder and was glued to either side of the Styrofoam sheets. Later, they were cut accordingly using hot wire running through the airfoil boundary.
- Then, the pieces formed were glued together so that each piece combined to give a single-wing structure. They were glued together using hot glue. Then, balsa wood was passed throughout the wing along its length to get the final wing structure. It was done to reinforce the wing and add strength to it while keeping the weight as light as possible.
- Once the main wing assembly was completed, plastic adhesive tape was carefully wrapped around the main wing to cover the outer surface of the wing to provide additional strength, rigidity, and waterproofing.
- The fuselage of the Glider was also made up of Styrofoam which was cut into the desired shape and size using the hot wire method. Two grooves

were created throughout the length of the body to reinforce the aluminum pipes making the body rigid. The elongation of the pipes was also used as the tail boom to attach vertical and horizontal stabilizers. The body was also wrapped with plastic adhesive tape to make it rigid and aerodynamically smooth.

5. The stabilizers were wrapped using plastic adhesive tape and glued together with the aluminum pipes that extended from the fuselage using hot glue.
6. The fuselage was made hollow in the front part to make a compartment for the battery, ESC, and other electronics.
7. The rear section of the wing was cut in the end area to arrange ailerons. The ailerons were attached with the help of tape. The arms from the servos were attached to control the horn of the aileron using steel wire.
8. Similarly, the elevators and rudders were also made in horizontal and vertical stabilizers which were attached to servos. The motor was mounted according to the puller-type configuration. The motor was attached in a plywood section which was mounted in the fuselage using hot glue.
9. Finally, all the basic electronics required for the manual flight were placed at their appropriate locations, i.e., servos, battery, ESC, and receiver as shown in Figure 7.



Figure 8: Final assembled glider

4.8. Avionics system design

Figure 9 depicts a block schematic of the controller's configuration. To summarize the flow chart, it starts

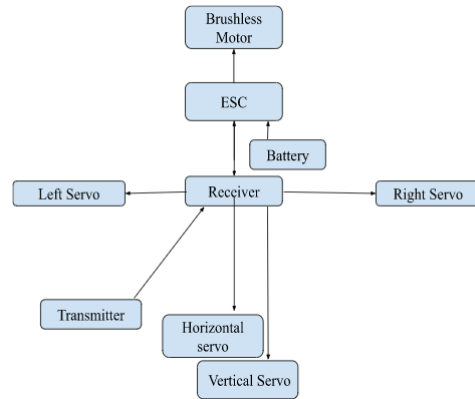


Figure 9: Flight control setup

with the battery delivering power, after that hardware components will initialize and boot. The flappers, rudder, and horizontal stabilizer will then be calibrated. After that, the receiver will begin checking the frequency and channels to ensure that it is properly linked to the transmitter.

4.9. Control system

The transmitter consists of 6 channels, for the better stability of the glider following control system was used. The available channels were used for the proper controlling of the glider as shown in the Figure 10.



Figure 10: Controller or transmitter

5. Results and discussion

The results from the design, simulation and analysis, fabrication, and testing of our Fixed Wing UAV are as follows:

5.1. Design

The wingspan of the UAV is 120 cm with a wing loading of 4.450 kg/m² with a gross weight of 805 grams. The body length of the UAV is 80 cm and the total length from the tip of the shaft to the tail edge of the elevator

is 90 cm. The location of the center of gravity is at the leading edge.

5.2. Calculation of Lift and Drag forces using XFLR software

The value of lift and drag coefficient were analyzed for the main wing in XFLR5 software under operating conditions. The method used for the analysis was a fixed speed type with a flight velocity of 10 m/s. The value of Reynold's number was calculated as below:

$$Re = \frac{\rho Lv}{\mu}$$

where, ρ = density of air = 1.225 kg/m³, L = length of chord = 15 cm, v = velocity of flight = 10 m/s, and μ = 1.4 × 10⁻⁵ m²/s. The value of Reynold's number is calculated as Re= 122500

1. For the main wing (NACA4415-unsymmetrical)

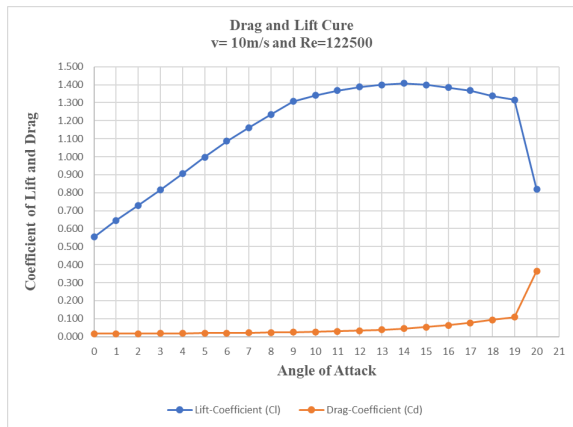


Figure 11: Drag and lift curve for the main wing

The maximum value of lift-coefficient of 1.408 and lift-force of 15.523 N is obtained at a 14-degree angle of attack. This point is called the stall point after which the lift force decreases, and the drag force increases as shown in Figure 11. It is possible to lift the glider before reaching the stall point. It is also found that the AOA of the wing should be about 4-5 degrees during the cruising phase to generate enough lift to keep the glider in the air. And found that the value of Cd increases with an increase in the AOA above the stall point.

2. For symmetrical wing (NACA0012)

For symmetrical airfoil, it is found that the coefficient of lift is increasing gradually which is required for the design.

Table 9: Drag and Lift Coefficient at different angle of attack

AOA (degree)	Lift-Coefficient (Cl)	Drag-Coefficient (Cd)	Lift Force (N)	Drag Force (N)
0	0.553	0.016	6.097	0.176
1	0.645	0.016	7.111	0.176
2	0.729	0.017	8.037	0.187
3	0.815	0.018	8.985	0.198
4	0.906	0.018	9.989	0.198
5	0.998	0.019	11.003	0.209
6	1.086	0.020	11.973	0.221
7	1.161	0.022	12.8	0.243
8	1.235	0.023	13.616	0.254
9	1.307	0.024	14.41	0.265
10	1.34	0.026	14.774	0.287
11	1.368	0.029	15.082	0.32
12	1.388	0.033	15.303	0.364
13	1.4	0.038	15.435	0.419
14	1.408	0.045	15.523	0.496
15	1.399	0.054	15.424	0.595
16	1.384	0.064	15.259	0.706
17	1.368	0.077	15.082	0.849
18	1.338	0.093	14.751	1.025
19	1.315	0.109	14.498	1.202
20	0.819	0.364	9.029	4.013

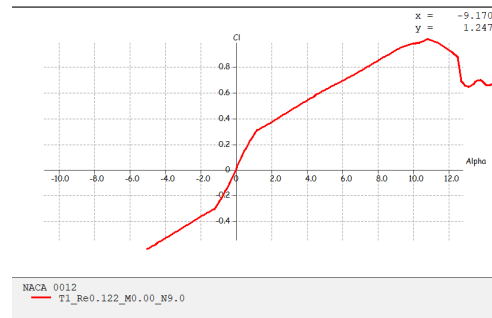


Figure 12: Lift curve for tail wing

3. CFD Analysis of the Main Wing:

To evaluate the aerodynamic performance of the designed UAV, a series of computational fluid dynamics simulations (CFD) were performed. For that purpose, the ANSYS Workbench 2021 R2

environment was used. The computational domain was created based on a profile of the airfoil. The airfoil was placed in the center of the domain (0,0,0) to seamlessly determine all desired coefficients. The airfoil was then subtracted using Boolean Tool, the remaining surface with the airfoil shape served as the air surrounding. The domain extends from +1.5m to -1m along X-axis, and +0.9m to -0.9m along Y-axis. The semicircular geometry of radius 0.9m was created for a better analysis of the airflow.

Such prepared geometry was transferred into ANSYS Meshing software. The mesh type was a 2D quadrilateral mesh with face meshing. To increase the quality of mesh the face meshing along with the mesh sizing was incorporated. The prepared computational domain was exported into Fluent Solver. Since low flight velocities (low Reynolds number) were to be simulated and therefore no sudden changes in pressure were expected, the pressure-based solver was chosen. To determine all force and moment coefficients the simulations were made in the steady state condition. All physicochemical properties of air were constant and averaged for the weather conditions at which the UAV will be tested.

Nowadays one may find publications in which CFD analysis of the UAVs is performed using the one-equation turbulence model (Spallart-Allmars) (One Equation Turbulence Models – CFD-Wiki, the Free CFD Reference,) or two-equation turbulence model (usually SST $k-\omega$) (Two Equation Turbulence Models – CFD-Wiki, the Free CFD Reference, n.d.). However, to achieve high accuracy of obtained results the four equation Transitional SST turbulence model was employed and a coupled pressure-velocity coupling algorithm was used. The major disadvantage of this decision was significantly longer times of calculations. The Langtry-Menter four-equation Transitional SST turbulence model (Langtry-Menter 4-Equation Transitional SST Model, n.d.) originates from the SST $k-\omega$ turbulence model. All discretization schemes were set to the second-order upwind whereas the gradients were evaluated using the Green-Gauss Node-Based method. As the convergence criteria the values of all scaled residuals smaller than $1e-06$ were assumed. The iterations were continued until these values did not achieve the constant level. The inlet for which direction vector and velocity magnitude were set. For the simulation velocity of magnitude 10m/s was used. The back surface of the domain was set as a pressure outlet. The

surface of the UAV was treated as a wall with no-slip condition. Finally, the remaining walls of the domain were set as walls with no-slip conditions. Following are the velocity and pressure contours at the different AOA (Angle of Attack).

(a) **Velocity and pressure contours at 0 degrees angle of attack**

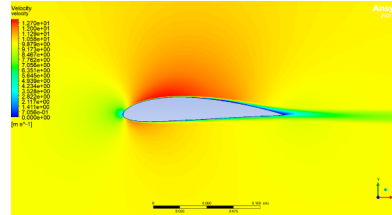


Figure 13: Velocity contour

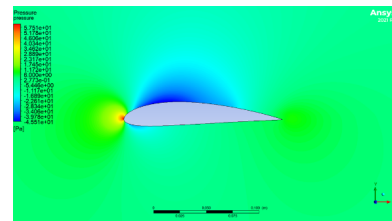


Figure 14: Pressure contour

(b) **Velocity and pressure contours at 5 degrees angle of attack**

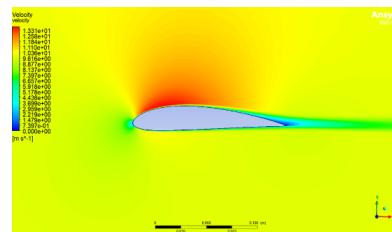


Figure 15: Velocity contour

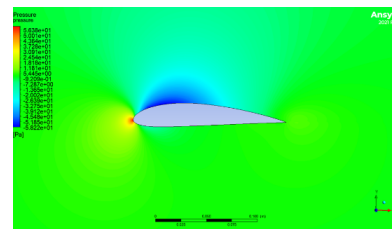


Figure 16: Pressure contour

(c) **Velocity and pressure contours at 14 degrees angle of attack**

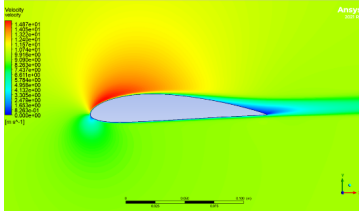


Figure 17: Velocity contour

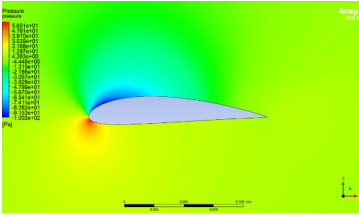


Figure 18: Pressure contour

It was found that, as the angle of attack was gradually increased, the boundary layer of air was getting separated from the fin surfaces at the tail edge. This boundary layer separation decreases the pressure gradient between the upper and lower faces of the foil and increases the drag force. This process of decreasing the pressure gradient with an increase in the angle of attack above the critical angle is called stalling, and the critical angle is called stall angle.

5.3. Static structural analysis of the main wing

The deflection study was done in the Static Structural Analysis system of the ANSYS Workbench. For the material properties of the Styrofoam following data were used.

Density = 25 kg/m³

Poisson's ratio = 0.05

Tensile Strength = 1.35 MPa

Yield Strength = 1 MPa

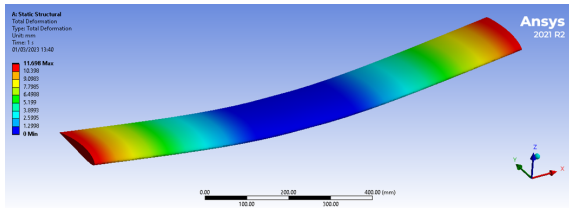


Figure 19: Total deflection of the main wing under maximum lift force

It has been found that the maximum deflection under

the maximum lift load of 15N is 11.69mm at the end of the wings as shown in Figure 19.

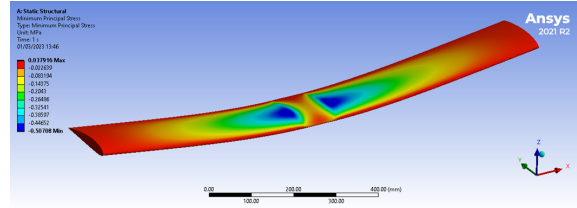


Figure 20: Maximum Principal Stress of the main wing under maximum lift force

The Maximum Principal stress (Tensile Stress) is found to be 0.075N, which is at the connection point between the wing and the fuselage as shown in Figure 20.

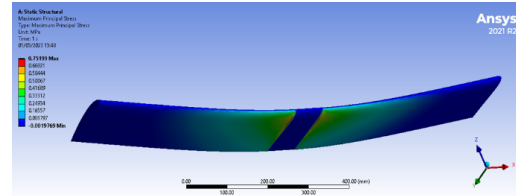


Figure 21: Minimum Principal Stress of the main wing under maximum lift force

The Minimum Principal stress (Compressive stress) is found to be -0.507N at the upper face of the wing at the connection point as in Figure 21. The value of stress is under the Yield strength and the Tensile strength of the material, so the design is safe from the view of stresses. The factor of safety can be calculated as:

$$FOS = \frac{\text{Ultimate tensile stress}}{\text{Maximum tensile stress}} = \frac{1.35}{0.75} = 1.8$$

The FOS is found to be 1.8 only, this value can be increased if the payload on the plane is decreased so that the maximum value of the lift force will be always below 15 N.

5.4. Theoretical glide ratio

- For the calculation of the Glide ratio, the MATLAB code was used to generate the flight trajectory under the following conditions:
- Weight of the glider: 800 g
 - Coefficient of lift at zero degrees: 0.553
 - Coefficient of drag at zero degree: 0.016
 - Initial velocity: 10 m/s
 - Surface area of the main wing: 0.18 m²
 - Initial vertical height: 100 m

Under the above-given conditions, the gliding trajectory of the glider was generated as shown in Figure 22. The horizontal distance traveled by the glider

would be approx. 350 m, which gave the glide ratio of about 3.5:1. This amount of glide is considerable for a UAV with an initial velocity in the range of 5-10 m/s.

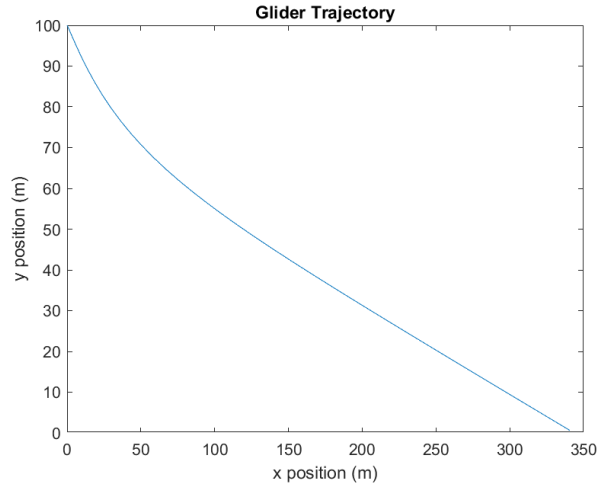


Figure 22: Gliding trajectory in MATLAB

5.5. Theoretical payload calculation

Payload is the amount of additional load that can be carried by a glider or a drone without affecting the flight conditions. From the airfoil analysis of the main wing, the maximum value of lift force was 15 N. From Table 6 and Table 7 the total mass of the glider is 801 grams. The payload was calculated as given in Table 10:

Table 10: Calculation of payload

S. N	Parameters	Value (gram)
1	Total weight	800
2	Lift load	1500
3	Payload	700

It will not be possible to fly the UAV with the payload calculated above, because the lift force will be just equal to the weight of the UAV, so the payload will not be equal to 700 grams, it has to be less than 700 grams. Considering the factor of safety, the payload can be from 100-200 grams so that the maximum value of lift force will always be below 15N.

5.6. Experimental thrust testing

The thrust testing was done in a digital weighing machine with a setup consisting of a motor and propeller. The values of current, voltage, and thrust at the corresponding speed of the motor were calculated in the Table 11.

From the Table 11 and Figure 23, it has been found that

Table 11: Experimental Thrust Testing

S. N	Seed (rpm)	Thrust (g)	Current (A)	Voltage (Volts)
1	0	0	0.1	11.5
2	1524	20	0.3	11.5
3	2500	46	0.56	11.3
4	3200	88	1	11.2
5	3800	157	1.3	11.2
6	4040	268	2.06	11.1
7	4570	296	2.51	11
8	4959	341	3.85	11
9	5040	460	5.38	10.9
10	5702	503	7.17	10.9
11	6300	586	10.1	10.6
12	8083	729	12.96	10.4
13	10090	893	13.67	10.1

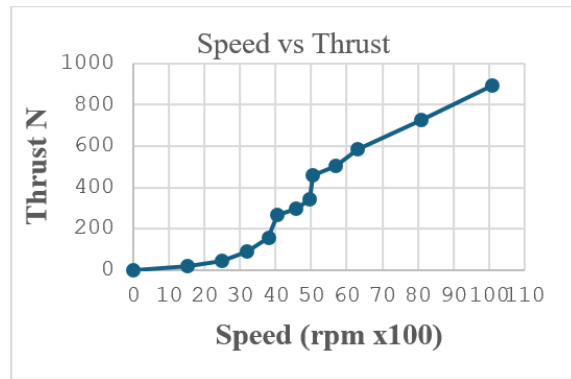


Figure 23: Thrust at different speeds of motor

thrust and current are increasing gradually with increasing in speed of the motor, but at the same time the value of voltage was decreasing. The speed of about 9000 rpm will be just able to pull the glider of load 800N.

5.7. Testing

The testing of the UAV was done in different phases and stages. The preliminary testing was done for the electronics parts, in the second phase testing was done for the gliding property and finally testing was done on the better stable and controlled flight of the UAV.

5.7.1. Preliminary testing

The preliminary testing was done to make sure that all the electronic parts were in their working condition and to test the static stability of the glider. The following testing was done in preliminary testing:

1. In the preliminary testing, the CG of the glider was tested. In this testing, it was found that the CG of the glider was about at the leading edge of

the main wing.

2. The rigidity of the glider was tested.
3. All the electronic parts were tested as:
 - (a) Calibration of the ESC and Servo motors.
 - (b) Proper orientation and the rotational direction of the brushless motor.

5.7.2. Testing of the gliding property

For the testing of the gliding property, the glider was launched without running motors and other electronics parts from a height of about 10ft with an initial velocity of about 9-10 m/s. Then the horizontal distance traveled by the glider was measured using the measuring tape and was found about 31ft from the point of the launch.

5.7.3. Endurance limit testing

For the testing of the endurance limit, the glider was tested on the ground with a propeller, during the thrust testing. The endurance limit of the glider was found to be about 9 minutes.



Figure 24: Successful flight testing

6. Conclusion and recommendation

6.1. Conclusion

As per the project objective, the efficient fixed-wing UAV was designed and fabricated by using available resources and technologies. The design and manufacturing of UAVs was entirely the work of engineering. The design specifications of the UAV were quite sensible and appropriate.

The design, simulation, and analysis of the UAV were done in the XFLR5, SOLIDWORKS, and ANSYS. The results obtained were compared and verified and found to be close to each other.

The UAV was equipped with the required electronics parts and the manual flight testing was done. The testing for the glide ratio was also done. The glide ratio was found to be about 3:1 which was almost the same as that of the theoretical value.

Therefore, all the project objectives were accomplished. However, there were some difficulties and shortcomings during the project. The recommendations for the shortcomings and betterment of the project are discussed in the succeeding topic.

6.2. Recommendation

The work presented here only focused on a small part of the issues that must be overcome to develop a viable solution for small, long-range unmanned vehicles. Based on the results and conclusion the following areas should be the focus in future work:

- Presently, there is wide use of composite material in the field of aviation. We can fabricate our UAV using composite material for better reinforcement, and surface finishing and prevent it from premature damage and crack propagation.
- The reinforcement of the wings can be done with composite fiber to increase the overall strength and decrease the weight.
- The stability of the UAV can be enhanced by using wings with a certain dihedral angle, and sweep angle.
- The range of our UAV can be increased using a wide-range flight controller system.
- Autonomous flight control systems can be incorporated for better experiences.
- Validation of the data obtained and results of the simulation and analysis can be done using other software. Hence, the outcome will be more reasonable and reliable.
- It will be better to include the experimental values of lift and drag coefficient from the wind tunnel testing.

Additionally, use of higher-grade electronics components, a large number of flight testing and optimization can be done for the better accomplishment of the project.

References

- [1] Bone E, Bolkcom C. Report for congress unmanned aerial vehicles[R]. Congressional Research Service, 2003: 1-52.
- [2] Fredericks W J, Moore M D, Busan R C. Benefits of hybrid-electric propulsion to achieve 4x increase in cruise efficiency for a vtol aircraft[C/OL]// 2013 International Powered Lift Conference. 2013: 1-21. DOI: [10.2514/6.2013-4324](https://doi.org/10.2514/6.2013-4324).
- [3] Traub L W. Range and endurance estimate for battery-powered aircraft[J/OL]. Journal of Aircraft, 2011, 48(2): 703-707. DOI: [10.2514/1.C031027](https://doi.org/10.2514/1.C031027).
- [4] Sunantyo A. Digital elevation model generated by unmanned aerial vehicle to determine available head assessment for micro hydro power plant in merawu river, banjarnegara district, central

- java[C]// Proceedings of the 3rd Applied Science for Technology Innovation, ASTECHNOVA 2014. 2014: 13-14.
- [5] Hieu N K, Loc H T. Airfoil selection for fixed wing of small unmanned aerial vehicles[M/OL]// Lecture Notes in Electrical Engineering: volume 371. 2016: 881-890. DOI: [10.1007/978-3-319-27247-4_73](https://doi.org/10.1007/978-3-319-27247-4_73).
- [6] Chang T, Yu H. Improving electric powered uavs' endurance by incorporating battery dumping concept[J/OL]. Procedia Engineering, 2015, 99: 168-179. DOI: [10.1016/j.proeng.2014.12.522](https://doi.org/10.1016/j.proeng.2014.12.522).
- [7] Alshehhi A, Almarar A, Alameri M, et al. Aerodynamic analysis of an airplane gliding in mars[C]// Proceedings of the International Astronautical Congress, IAC: volume 5. 2017: 2767-2778.
- [8] Escobar-Ruiz A G, Lopez-Botello O, Reyes-Osorio L, et al. Conceptual design of an unmanned fixed-wing aerial vehicle based on alternative energy[J/OL]. International Journal of Aerospace Engineering, 2019. DOI: [10.1155/2019/8104927](https://doi.org/10.1155/2019/8104927).
- [9] Keskİn G, Durmuş S, Kafalı H. The developments in electric-powered motor gliders[J]. 2019.
- [10] Laksham K. Unmanned aerial vehicle (drones) in public health: A swot analysis[J/OL]. Journal of Family Medicine and Primary Care, 2019, 8(2): 342. DOI: [10.4103/jfmpe.jfmpe_413_18](https://doi.org/10.4103/jfmpe.jfmpe_413_18).
- [11] Kozuba J, Wojnar T, Mrozik M, et al. Use of electric motors in the context of glider aviation[J/OL]. Journal of KONBiN, 2021, 51(2): 103-115. DOI: [10.2478/jok-2021-0025](https://doi.org/10.2478/jok-2021-0025).
- [12] Fouatih O M, Medale M, Imine O, et al. Design optimization of the aerodynamic passive flow control on naca 4415 airfoil using vortex generators[J/OL]. European Journal of Mechanics, B/Fluids, 2016, 56: 82-96. DOI: [10.1016/j.euromechflu.2015.11.006](https://doi.org/10.1016/j.euromechflu.2015.11.006).
- [13] McCroskey W J. A critical assessment of wind tunnel results for the naca 0012 airfoil[R]. NASA Technical Memorandum 100019 USAAVSCOM Technical Report 87-A-5, 1987.